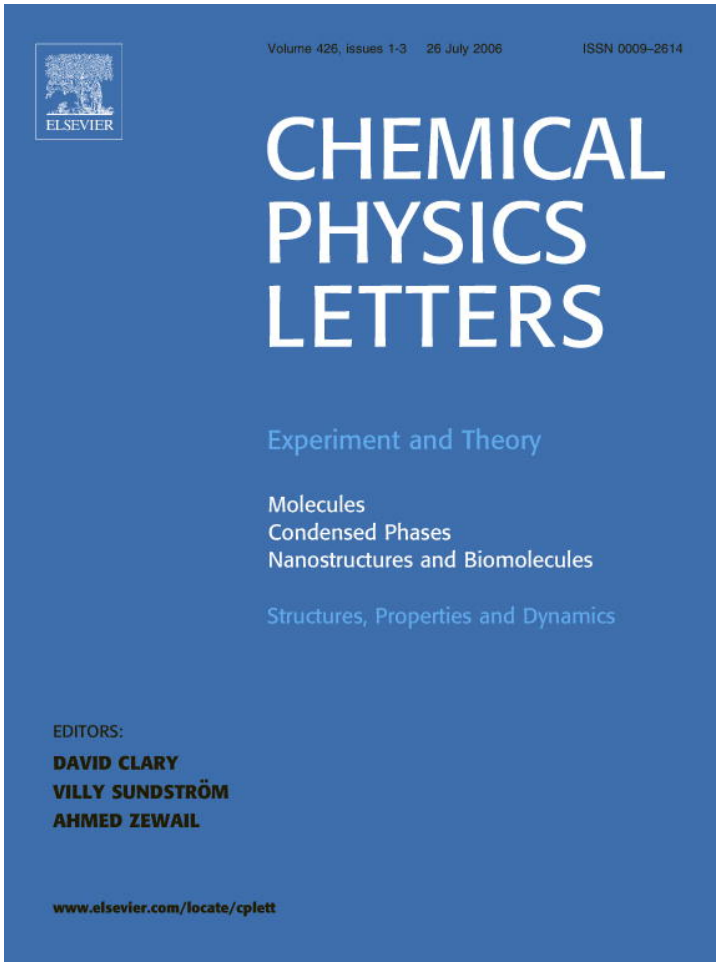

Available online at www.sciencedirect.com
SCIENCE DIRECT®
Chemical Physics Letters 426 (2006) 187–191
CHEMICAL PHYSICS LETTERS
www.elsevier.com/locate/cplett

Multiple-quantum ^{13}C solid-state NMR spectroscopy under moderate magic-angle spinning

Sungsool Wi [a,*], Son-Jong Hwang [b]

[a] Department of Chemistry, Virginia Tech, Blacksburg, VA 24061, USA
[b] The Division of Chemistry and Chemical Engineering, California Institute of Technology, Pasadena, CA 91125, USA

Received 31 March 2006; in final form 18 May 2006
Available online 3 June 2006

Abstract

A new method for the excitation and detection of high-order ^{13}C multiple-quantum (MQ) nuclear magnetic resonance (NMR) signals in solids under magic-angle spinning (MAS) condition is presented. In this experimental scheme, high-order ^{13}C MQ coherences are generated by relaying several sequentially generated ^{13}C double-quantum (DQ) coherences in dipolar coupled networks. Numerical simulations and experimental implementations are presented to demonstrate the efficiency of this method under a moderate MAS frequency regime. ^{13}C MQ signals up to 10-quantum coherences are observed experimentally on the model compound 1-^{13}C-labeled glycine, at an MAS frequency of 12 kHz.

1. Introduction

Multiple-quantum (MQ) NMR spectroscopy has been developed as a valuable tool for estimating the size and topology of localized nuclear spin clusters in solids [1–6]. Numerous examples of static MQ NMR applications have been reported for spin clusters of large magnetic moment nuclei, such as ^{1}H or ^{19}F, which provide homogeneously broadened line shapes [7–11] as well as for spin clusters of small magnetic moment nuclei, such as ^{13}C, which provide inhomogeneously broadened line shapes [12–14].

It is highly desirable to combine MQ spectroscopy with magic-angle spinning (MAS) in order to improve the spectral resolution and sensitivity. MQ ^{1}H NMR techniques under MAS have been reported by Meier and Earl [15], Ba and Veeman [16], Ding and McDowell [17], and Spiess and coworkers [18]. But, all these methods are still not suitable for ^{13}C MQ NMR spectroscopy because of the inherent difficulty to generate a time-reversible effective ^{13}C–^{13}C dipolar coupling in the presence of large offset differences and chemical shift anisotropies (CSA).

^{13}C MQ spectroscopy using symmetry-based homonuclear dipolar recoupling sequences [19–21], which effectively suppress the large offset difference and CSA, have been demonstrated by Levitt and co-workers [22–24] and Edén and Brinkmann [25]. In these approaches MQ coherences are built up by the so-called second-order recoupling terms, therefore, ^{13}C MQ signals higher than double-quantum (DQ) coherence are very low. According to the average Hamiltonian Theory (AHT), MQ coherences arise from higher-order cross-terms between operators from two spin interactions. Oyler and Tycko developed an efficient ^{13}C MQ NMR technique [26] by utilizing the finite pulse effect of radio-frequency-driven recoupling (fpRFDR) sequence [27] under fast MAS frequencies ($20 \sim 30$ kHz). This method produces a pseudo-static dipole–dipole Hamiltonian with time trajectory that is partially reversible by a phase altered reconversion mixing pulse.

Here, we present an alternative route to generate high-order ^{13}C MQ signals by relaying the spin clusters sequentially under the influences of pairwise ^{13}C–^{13}C DQ Hamiltonians. For this purpose, symmetry-based dipolar DQ recoupling sequences developed by Levitt and coworkers [19,20] have been concatenated by $\pi/2$ pulses. This approach differs from the previous approaches by Levitt

* Corresponding author. Fax: +1 540 231 3255.
E-mail address: sungsool@vt.edu (S. Wi).

0009-2614/$ - see front matter © 2006 Elsevier B.V. All rights reserved.
doi:10.1016/j.cplett.2006.05.097

and co-workers and Edén and Brinkmann that it generates every order of MQ coherences within the zero-order of AHT. This method opens up a new avenue to produce high-order ^{13}C MQ signals efficiently under a moderate MAS frequency regime.

2. Theoretical consideration

DQ recoupling pulses. A family of symmetry-based broadband DQ recoupling sequences SRN_n^v [19,20] is incorporated as a basic pulse unit to be relayed. The SRN_n^v family produces an effective dipole–dipole DQ Hamiltonian under MAS even in the presence of large CSA, offset difference, and radio-frequency (rf) inhomogeniety. The SRN_n^v pulse sequence consists of

$$SRN_n^v = [RN_n^v \cdot RN_n^{-v}]_l; \quad RN_n^v = [90_\phi 270_{\phi+\pi} 90_{-\phi} 270_{-\phi+\pi}]_{N/2}; \quad l = 1, 2, \ldots, \tag{1}$$

where n, v, and N are integers designating spinning rotor period, rf phase rotation with phase $\phi = v\pi/N$, and repetitions of the basic RN_n^v element ($\equiv 90_{\pm\phi}270_{\pm\phi+\pi}$) of duration τ_C ($\tau_C = n\tau_r/N$, where $\tau_r = |2\pi/\omega_r|$ is the rotation period and ω_r is the sample rotation frequency), respectively. A single RN_n^v block occupies n rotor periods with a rf amplitude $\omega_{rf} = N\omega_r/n$.

Generation of MQ coherences. Sequential concatenation of pairwise DQ coherences can generate high-order MQ coherences in solids under MAS. This reminds the creation of high-order MQ coherences via the through-bond J-couplings in liquid state [28]. Similarly, Carravetta et al. [29] demonstrated that triple-quantum coherences can be generated efficiently by combining selective DQ excitation with rotational resonance for ^{13}C MAS NMR. The idea of creating MQ coherences via the pairwise concatenations of DQ coherences is depicted in Fig. 1. We assume a three-spin system 1–2–3, in which the spin pairs 1–2 and 2–3 have measurable dipolar couplings whereas the spin pair 1–3 has a negligible dipolar interaction. In order to further simplify

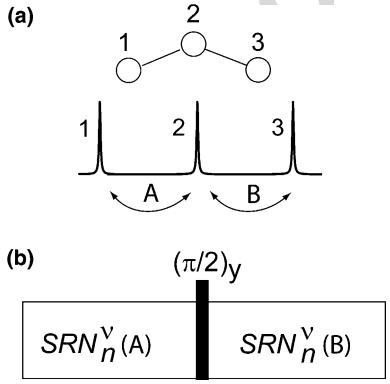

Fig. 1. (a) A model spin system, the atom numbering and the spectrum. (b) Two separate blocks of the homonuclear dipolar DQ recoupling pulse SRN_n^v are relayed by a 90° degree pulse. It is assumed that the first and the second SRN_n^v blocks reintroduce dipolar coupling A along the spin pair 1–2 and B along the spin pair 2–3, respectively.

the system we make a second assumption that the first DQ recoupling sequence works selectively on the spin pair 1–2 and the second block works only on the spin pair 2–3, respectively. Spins are initially in the longitudinal mode $I_{z,ij}^{1-4}$ $(i, j = 1, 2, 3.)$. Upon the action of the first dipolar DQ recoupling sequence, the $I_{z,12}^{1-4}$ $(\equiv I_{1z} + I_{2z})$ state is converted into an effective DQ coherence $I_{y,12}^{1-4}$:

$$e^{-i2\pi\tau v_{12} I_{x,12}^{1-4}} I_{z,12}^{1-4} e^{i2\pi\tau v_{12} I_{x,12}^{1-4}} = I_{y,12}^{1-4}; \quad \tau \approx 1/4v_{12}, \tag{2}$$

where $I_{x,12}^{1-4} \equiv [I_{1x}I_{2x} - I_{1y}I_{2y}]$, $I_{y,12}^{1-4} \equiv [I_{1y}I_{2x} + I_{1x}I_{2y}]$. The effective dipolar coupling strength v_{12} between spin pair 1–2 depends on the dipolar coupling strength, the orientation of the internuclear vector of spin 1 and 2, and the scaling factor of the SRN_n^v sequence [19,20].

A 90° pulse along the y axis converts the $I_{y,12}^{1-4}$ term into a single-quantum anti-phase coherence $I_{1y}I_{2z} + I_{1z}I_{2y}$ by flipping I_x into I_z, while leaving I_y unchanged. The evolution of the $I_{1y}I_{2z}$ term during the second SRN_n^v block builds up an effective DQ coherence along the spin pair 2–3, producing coherences, including the triple-quantum coherence:

$$e^{-i2\pi\tau v_{23} I_{x,23}^{1-4}} [I_{1y}I_{2z} + I_{3z}] e^{i2\pi\tau v_{23} I_{x,23}^{1-4}} = I_{1y}(I_{2y}I_{3x} + I_{2x}I_{3y}); \quad \tau \approx 1/4v_{23}. \tag{3}$$

In general, all previous assumptions made should be removed, and the evolution of the density matrix under every SRN_n^v block after the first one becomes very complicated due to the non-commuting nature of any two dipolar Hamiltonians that share a common spin in dipolar couplings as below:

$$[v_{ij} I_{x,ij}^{1-4}, v_{jk} I_{x,jk}^{1-4}] = v_{ij} \cdot v_{jk}(I_{iy}I_{jz}I_{kx} - I_{ix}I_{jz}I_{ky}) \neq 0. \tag{4}$$

To analyze the generations of various orders of MQ coherences, a numerical calculation based on the density matrix propagations must be carried out. For a n-spin coupled system that is under influences of k $SRN_n^v(\Phi_k)$ blocks and $(k-1)$ $90°_{y+\Phi_k}$ pulses, the density matrix evolution of each quantum coherence can be calculated by exact time propagations:

$$\mathrm{Tr}(I_\lambda \cdot U_k \ldots PU_2PU_1\{I_{1z} + I_{2z} + I_{3z} + \ldots + I_{nz}\}U_1^{-1}P^{-1}U_2^{-1}P^{-1}\ldots U_k^{-1}), \tag{5}$$

where $U_l \equiv \exp\left\{-i2\pi\tau_l \sum_{i<j}^{n} v_{ij}\left(I_{x,ij}^{1-4}\cos\Phi_k + I_{y,ij}^{1-4}\sin\Phi_k\right)\right\}$, $P = \exp\left\{-i\left(\frac{\pi}{2}\right)I_{y+\Phi_k}\right\}$, λ is the order of each quantum coherence, and Φ_k is SRN_n^v pulse phase angle.

3. Experiments and simulations

MQ sequence consideration. Fig. 2a shows the sequence used in our ^{13}C MQ NMR experiments. ^{13}C magnetizations are prepared by cross-polarization (CP) from ^{1}H nuclei and then transferred into longitudinal components by a $\pi/2$ pulse. Residual transverse magnetizations dephase during the delay τ (~2 ms) with no ^{1}H decoupling. Longitudinal magnetizations are fed into the MQ excitation period, which consists of multiple SRN_n^v blocks and 90° pulses

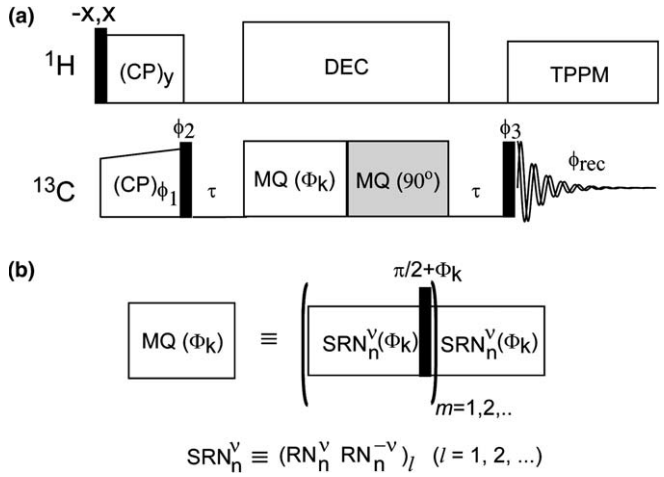

Fig. 2. Pulse sequence for ^{13}C MQ MAS NMR spectroscopy. (a) Overall sequence, demonstrating the generation of ^{13}C magnetization from cross-polarization (CP), dephasing period τ, MQ excitation and mixing periods, and signal detection period t_2. Phase cycling: $\phi_1 = 0, 0, 1, 1, 2, 2, 3, 3$; $\phi_2 = 1, 3, 2, 0, 3, 1, 0, 2$; $\phi_3 = 3, 1, 0, 2, 1, 3, 2, 0$; $\phi_{rec} = 0, 0, 1, 1, 2, 2, 3, 3$. (b) The MQ pulse unit used in MQ preparation and mixing periods.

(black bars) as shown in the Fig. 2b, with an overall rf phase shift Φ_k applied for $\tau_{MQ} = 2nl(m+1)\tau_r$, where l and m are integers determining the length of SRN_n^ν supercycle and the repetitions of overall relay, respectively. The following MQ mixing period whose phase is shifted by an overall phase shift $\pi/2$ from the MQ excitation period reconverts various MQ coherences to z-orders of magnetization. After a second z-filtering period τ, ^{13}C MQ coherence signals are detected during the t_2 period after a $\pi/2$ read pulse. An alternating pulse phase between 0° and 180° is incorporated for the last $\pi/2$ read pulse to remove the signal contributions from the magnetizations that may develop during τ through T_1 relaxation. Two-dimensional (2D) time proportional phase-increment (TPPI) data sets $S(\Phi_k, t_2)$ are acquired with phase shifts $\Phi_k = (2\pi k/N)$, $k = 0, 1, 2, \ldots, N-1$ [6].

Sample preparation and NMR spectroscopy. Polycrystalline 1-^{13}C-Gly was purchased from Cambridge Isotopes laboratories and used without further purifications. Natural abundance glycine was purchased from Sigma Chemical Co. A 25% 1-^{13}C-labeled glycine sample was recrystallized from the corresponding mixture of natural abundant and 1-^{13}C-labeled glycines in water at room temperature.

NMR experiments were performed on a Bruker DSX-500 spectrometer operating at a ^{1}H frequency of 500.23 MHz and ^{13}C frequency at 125.80 MHz, using a Bruker 4.0 mm MAS NMR probe. Cross-polarization was achieved at 50 kHz rf field at the ^{1}H channel and by linearly ramping the ^{13}C rf field over a 25% range centered at 38 kHz. Proton decoupling powers during the MQ excitation/mixing periods and the signal detection period (TPPM decoupling) were 110 KHz and 71 kHz, respectively. The duration of carbon 90° pulse was 5 μs. $SR14_4^5$-based MQ excitation and mixing units were employed at a 12 kHz MAS frequency. The pulse power of $SR14_4^5$ block was optimized experimentally around the theoretically expected value (=3.5 ω_r).

Simulations of ^{13}C MQ NMR spectra. Brute-force calculations were carried out using a home-built MATLAB program developed in-house based on full density matrix evolutions under the influences of the pulses in the sequence (see Fig. 2). The program code produces all orders of MQ coherences at the end of the MQ excitation period. Each order of MQ coherence thus generated is fed separately into the MQ mixing period to be converted into z-order, and the sampling takes place during t_2 after a 90° read pulse. Only the first data point of FID during t_2 was considered to save time. All the relevant internal Hamiltonians are considered explicitly and are approximated as piecewise-constants with 56 increments per rotor period. The simulation assumed a 11.75 T magnetic field, a 10 kHz spinning speed, a 65 kHz rf pulse amplitude for $SR26_4^{11}$ sequence, and a 3.5 μs 90° pulse. A three-angle set of 538 crystallite orientations generated by the Conroy method [30] was employed for powder averages.

Fig. 3 shows simulated MQ excitation profiles of five-spin ^{13}C clusters of linear, square planar, and tetrahedral bipyramidal geometries at three different τ_{MQ}s: 3.2 ms ($m = 1$, and $l = 2$), 7.2 ms ($m = 2$, and $l = 3$) and 9.6 ms

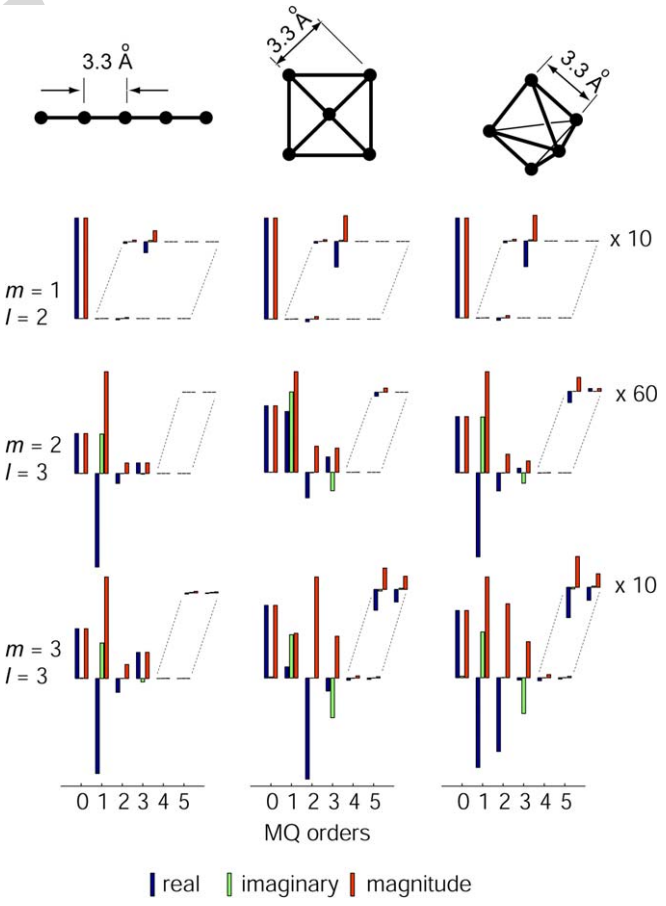

Fig. 3. Simulated MQ signal amplitudes of various geometries of five-spin systems. See the text for the details of simulation parameters. The relative intensities of the MQ signals increase as the τ_{MQ} increases.

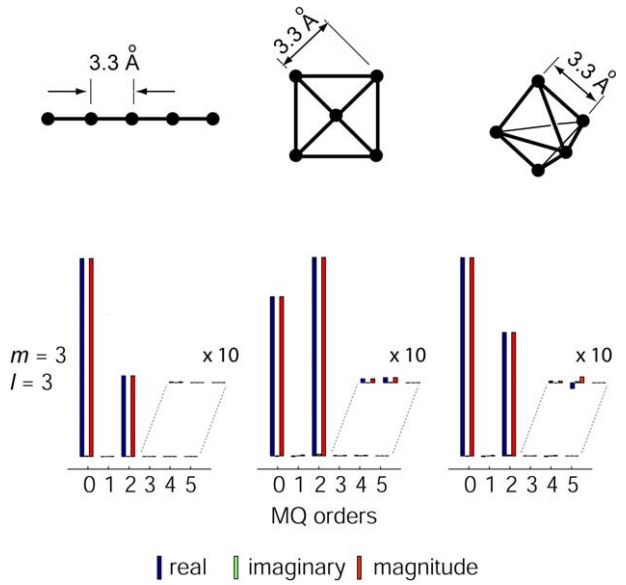

Fig. 4. Idem as in Fig. 3 but by omitting the 90° degree pulses from the MQ sequence block, with $m = 3$ and $l = 3$.

($m = 3$, and $l = 3$). The nearest ^{13}C–^{13}C distance in each model is 3.3 Å and a 71 ppm of CSA with an asymmetric parameter $\eta = 0.85$ was assumed for each carbon site at the zero offset frequency. The z-directions of the CSA tensor orientations are coinciding to the dipolar vectors (linear model), perpendicular to the square plane (square planar model), and collinear to the main C_3 axis (tetrahedral bipyramid model). Signals for the central atom of linear and square planar models have been sampled to minimize edge effects. MQ intensity profiles thus obtained (Fig. 3) show strong dependences on the mixing time τ_{MQ}, and are sensitive to the topology of spin systems. The appearance of the imaginary MQ signals is a manifestation of imperfections in the time-reversibility of the overall pulse sequence. Relative amplitudes of four- and five-quantum signals are low, probably due to the low probabilities of possible four- and five-quantum transitions. When a MQ sequence block without the 90° degree pulses, a basic SRN_n^v sequence, is considered, it relies on the high-order cross-terms between operators from two spin interactions to excite high-order MQ coherences, therefore, the signal amplitudes of high-order MQ coherences thus generated would be extremely low compared to those from zero- and double-quantum coherences even at a long τ_{MQ} ($m = 3$, and $l = 3$) (Fig. 4).

4. Results and discussion

Fig. 5 shows experimentally measured ^{13}C MQ excitation NMR spectra of natural abundant (a, and d), 25 % 1-^{13}C-labeled (b, and e), and 100% 1-^{13}C-labeled (c, and f) glycine samples at two different τ_{MQ}s: 4 ms ($l = 2$, $m = 2$; a, b, and c) and 10 ms ($l = 3$, $m = 4$; d, e, and f). The MQ coherences generated are shown by numbers on the bottom axis of the spectra. Each trace represents the probability amplitude for excitation and detection of nth quantum coherence as a function of single-quantum NMR frequency measured during t_2. The natural abundance sample shows coherences only up to 2-quanta even at $\tau_{MQ} = 10$ ms (Fig. 5d), while the labeled samples evidence higher-order MQ coherences for both τ_{MQ}s. Particularly, as shown in Fig. 5f, a coherent superposition of spin states involving a correlation of spin angular momenta of at least 10 different ^{13}C nuclei has been excited and detected at $\tau_{MQ} = 10$ ms for the 100% 1-^{13}C-labeled sample. The nearest-neighbor distances among ^{13}C labels are 3.39 Å in the crystal lattice of 1-^{13}C L-glycine [31]. As predicted in the simulations, every order of MQ coherence is observed experimentally although our sequence resembles the so-called 2-spin 2-quantum propagator [3].

This method might be an extreme case of the HSMAS-MQ method [26] because the finite pulse effect of the applied rf pulses are maximized (windowless). As in the

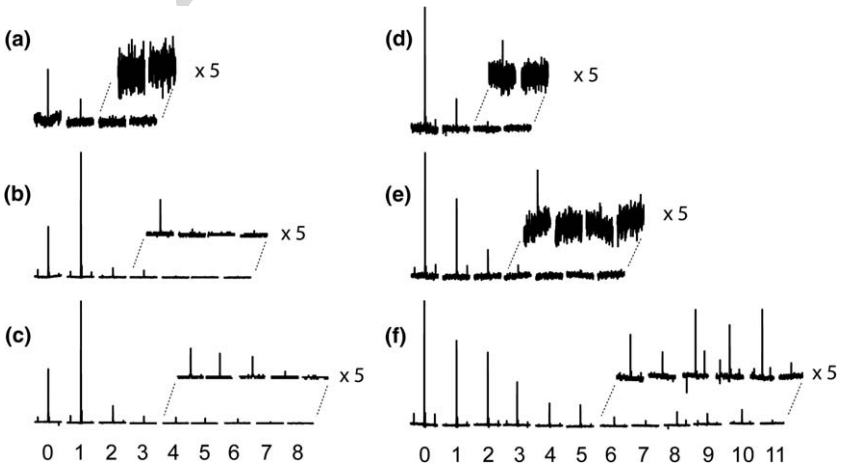

Fig. 5. Side-by-side plots of phase-adjusted real parts of the experimental ^{13}C MQ NMR spectra of 1-^{13}C-glycine obtained at 125.8 MHz with 32 increments in Φ_k and 32 scans (c, and f), 64 scans (b, and e), and 128 scans (a, and d) per Φ_k value. Results are shown for natural abundance (a, and d), 25% 1-^{13}C-labeled (b, and e), and 100% 1-^{13}C-labeled (c, and f) glycines with 4 ms (a, b, and c) and 10 ms (d, e, and f) of τ_{MQ}s. Spinning speed was 12 kHz. The rf pulse amplitudes of 90° pulses, $SR14_4^5$ blocks, and CP spin-lock were 50 kHz, 42 kHz, and 50 kHz respectively. Proton decoupling powers for $SR14_4^5$ blocks and for the direct acquisition period were 110 kHz and 71 kHz, respectively.

case of HSMAS-MQ method, our pulse technique fulfills time-reversal property at least partially as proven by the observations of the nondestructive MQ signals. However, imperfections in time-reversal property are manifested by the observations of the imaginary part of MQ spectrum.

The minimum phase setting time (~2 μs) required at our spectrometer console, which was found experimentally during the optimization of our MQ sequence, imposed limitations for the implementation of a $R26_4^{11}$-based sequence at the 12 kHz spinning speed because of the limited pulse window sizes associated with. However, the $R26_4^{11}$-based technique provided better MQ excitation profiles over the $SR14_4^5$-based sequence in our simulations. A better ^{13}C MQ experiment would be obtained by a modern rf console that provides a shorter phase setting time.

An alternative ^{13}C MQ pulse scheme was also tested by preparing a transverse mode of magnetizations by placing 45° pulses before and after the MQ excitation and mixing blocks. This approach allowed generation of ^{13}C MQ NMR signals in a comparable quality to the original longitudinal mode (data not shown).

5. Conclusion

An effective way to generate high-order ^{13}C MQ coherences under a moderate MAS spinning frequency is implemented by concatenating several pairwisely generated dipolar DQ Hamiltonians. Symmetry-based dipolar DQ recoupling sequences have been relayed to generate ^{13}C MQ coherences, even in the presence of large offsets, CSAs, and ^{13}C-^{1}H couplings. A fast MAS cannot be often achieved in practical solid-state NMR experiments on membrane associated peptides and proteins since they are subject to water and lipid phase separations. Thus, this method may be particularly useful in structural and functional studies of such biological systems that can be neither solubilized nor crystallized.

Appendix A. Supplementary data

Supplementary data associated with this article can be found, in the online version, at doi:10.1016/j.cplett.2006.05.097.

References

[1] J. Baum, M. Munowitz, A.N. Garroway, A. Pines, J. Chem. Phys. 83 (1985) 2015.
[2] Y.S. Yen, A. Pines, J. Chem. Phys. 78 (1983) 3579.
[3] J. Baum, A. Pines, J. Am. Chem. Soc. 108 (1986) 7447.
[4] W.V. Gerasimowicz, A.N. Garroway, J.B. Miller, J. Am. Chem. Soc. 112 (1990) 3726.
[5] D. Suter, S.B. Liu, J. Baum, A. Pines, Chem. Phys. 114 (1987) 103.
[6] D.N. Shykind, J. Baum, S.B. Liu, A. Pines, J. Magn. Reson. 76 (1988) 149.
[7] J. Baum, K.K. Gleason, A. Pines, A.N. Garroway, J.A. Reimer, Phys. Rev. Lett. 56 (1986) 1377.
[8] M.A. Petrich, K.K. Gleason, J.A. Reimer, Phys. Rev. B 36 (1987) 9722.
[9] D.H. Levy, K.K. Gleason, J. Phys. Chem. 96 (1992) 8125.
[10] S.J. Hwang, D.O. Uner, T.S. King, M. Pruski, B.C. Gerstein, J. Phys. Chem. 99 (1995) 3697.
[11] S.J. Limb, B.E. Scruggs, K.K. Gleason, Macromolecules 26 (1993) 3750.
[12] O.N. Antzutkin, Magn. Reson. Chem. 42 (2004) 231.
[13] O.N. Antzutkin, J.J. Balbach, R.D. Leapman, N.W. Rizzo, J. Reed, R. Tycko, Proc. Natl. Acad. Sci. USA 97 (2000) 13045.
[14] O.N. Antzutkin, R. Tycko, J. Chem. Phys. 110 (1999) 2749.
[15] B.H. Meier, W.L. Earl, J. Chem. Phys. 85 (1986) 4905.
[16] Y. Ba, W.S. Veeman, Solid-State NMR 3 (1994) 249.
[17] S.W. Ding, C.A. McDowell, J. Magn. Reson., Ser. A 120 (1996) 261.
[18] H. Geen, R. Graf, A.S.D. Heindrichs, B.S. Hickman, I. Schnell, H.W. Spiess, J.J. Titman, J. Magn. Reson. 138 (1999) 167.
[19] A. Brinkmann, M.H. Levitt, J. Chem. Phys. 115 (2001) 357.
[20] M. Carravetta, M. Edén, X. Zhao, A. Brinkmann, M.H. Levitt, Chem. Phys. Lett. 321 (2000) 205.
[21] Y.K. Lee, N.D. Kurur, M. Helmle, O.G. Johannessen, N.C. Nielsen, M.H. Levitt, Chem. Phys. Lett. 242 (1995) 304.
[22] C.E. Hughes, J.S.A.D. Gunne, M.H. Levitt, ChemPhysChem 4 (2003) 457.
[23] M. Edén, M.H. Levitt, Chem. Phys. Lett. 293 (1998) 173.
[24] J.D. van Beek, M. Carravetta, G.C. Antonioli, M.H. Levitt, J. Chem. Phys. 122 (2005) 224510.
[25] M. Edén, A. Brinkmann, J. Magn. Reson. 173 (2005) 259.
[26] N.A. Oyler, R. Tycko, J. Phys. Chem. B 106 (2002) 8382.
[27] Y. Ishii, J. Chem. Phys. 114 (2001) 8473.
[28] R.R. Ernst, G. Bodenhausen, A. Wokaun, Principles of Nuclear Magnetic Resonance in One and Two Dimensions, Oxford, New York, 1987.
[29] M. Carravetta, J.S. auf der Gunne, M.H. Levitt, J. Magn. Reson. 162 (2003) 443.
[30] Available from: <http://www.mhl.soton.ac.uk/public/software/Orientations/index.html>.
[31] R.E. Marsh, Acta Cryst. 11 (1958) 654.